Transactions, SMiRT-26
Berlin/Potsdam, Germany, July 10-15, 2022
Division I

CREEP EFFECTS IN PRESTRESSED CONCRETE CONTAINMENT VESSELS

Daniel Parker[1], Randy James[2]

[1] Senior Consultant, Structural Integrity Associates, Inc., San Diego, CA, USA (dparker@structint.com)
[2] Principal, Structural Solutions Consulting, LLC., San Diego, CA, USA

ABSTRACT

This paper presents a brief study to examine the issue of creep in prestressed concrete containment vessels. A portion of a representative containment structure is modeled where a steel liner, tendons, and nominal reinforcement steel is explicitly modeled. A constitutive material model, ANACAP, coupled with the ABAQUS general purpose finite element program is utilized to perform the analyses modeling the effect of concrete creep, creep recovery, and cracking. The analyses are time-dependent and include a detensioning step where a handful of stressed tendons are removed after three decades of creep. Several inputs are varied within the study including the concrete fracture strain, creep compliance, differential creep, time dependency of material properties, and tendon removal sequence. Two primary findings are identified: (1) the calculated radial strain profile after detensioning is significantly different if creep is included in the analysis and the profile with creep included better resembles the hourglass shape found in the delamination cracking observed at Crystal River; and (2) specific tendon removal sequences show an increase in mechanical (radial) strain during detensioning and an increase in total radial strain during creep recovery. Other observations and recommended future studies are discussed. The results from this paper will be useful to engineers interested in accounting for creep in structural assessments, facility owners with prestressed or post-tensioned concrete structures, and academics interested in modeling creep analytically.

INTRODUCTION

The effects of creep on the long-term integrity of Prestressed Concrete Containment Vessels (PCCVs) are complicated and not intricately analyzed by structural engineers. While creep is included in the design basis for pre-stress loss in PCCVs, the long-term effects on the structural integrity have not been critically studied. The general sense has been that creep is mostly a shorter-term effect, and the effects of creep should decrease over time as the structure ages and the rate of creep dissipates. However, the delamination cracking that developed in the containment at Crystal River, Figure 1, during a construction modification raised concerns about the possible longer-term effects of creep, especially when there are changes in the loading. Research is needed to further investigate the effects of creep and identify situations where the integrity and pressure capacity of PCCVs may or may not be of some concern in the longer term.

As a collaborative effort, Structural Integrity Associates (SI) and Structural Solutions Consultants (SSC) performed a limited scope study to examine the issue of creep in concrete containment vessels and identify any need for further research. This work consisted of a series of nonlinear finite element analyses (FEA) to evaluate different scenarios including possible existing defects, variations of fracture properties and creep compliance, and de-tensioning sequence of groups of tendons in order to understand the sensitivity of each variable on the creep response of the PCCV. In practice, concrete material properties change over time. Excluding degradation due to numerous environmental factors, concrete increases in strength and elastic modulus as it ages. Although commonly designs are based on the 28-day material properties; this study included the effects of time-dependent material properties in a representative aging

PCCV. The analyses were performed with the ABAQUS general purpose finite element program coupled with SIA's proprietary concrete constitutive model, ANACAP.

This effort is not an attempt to reconstruct all the circumstances that occurred in the Crystal River delamination problem as a kind of "root cause" analysis. Rather, the intent is to consider representative conditions for a situation where a known problem develops in order to show that the modeling employed can provide an indication of potential problems.

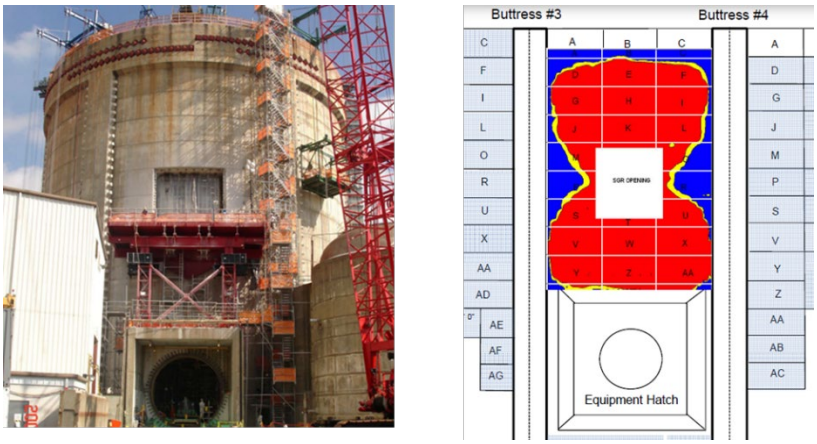

Figure 1 Crystal River Structure (Left) and Extent of Delamination (Right)

ANACAP CONCRETE CONSTITUTIVE MODEL

The analyses utilize ANACAP, SI's proprietary concrete model. A thorough description of ANACAP's features is not presented herein, but a brief discussion of tensile cracking is warranted. Tensile cracking in ANACAP is governed by the magnitude of the load in the directions of principal strain. Cracks are assumed to form perpendicular to the directions of largest tensile strains. Multiple cracks are allowed to form at each material point, but they are constrained to be mutually orthogonal. If cracking occurs, the normal stress across the crack is reduced to zero and the distribution of stresses around the crack is recalculated through equilibrium iterations. This allows stress redistribution and load transfer to reinforcement or other load paths in the structure. Once a crack forms, the direction of the crack remains fixed and can never change or heal. However, a crack can close, resist compression and shear, and re-open under load reversals. The cracking criterion is based on an interaction of both stress and strain as illustrated in Figure 2. The model predicts cracking when the generalized (principal) stress and strain state exceeds the limit state shown. Thus, biaxial and triaxial stress states are treated consistently with uniaxial conditions, but the associated cracking will now occur at a slightly higher stress and slightly lower strain. Split cracking, for example near a free edge under high compressive stress, occurs at near zero stress and a tensile strain approximately twice that of uniaxial tensile cracking.

Commonly, the continuing hydration of concrete over time results in time dependent concrete mechanical properties. The material model can consider both static and/or time-dependent mechanical properties such as modulus of elasticity, creep and shrinkage effects.

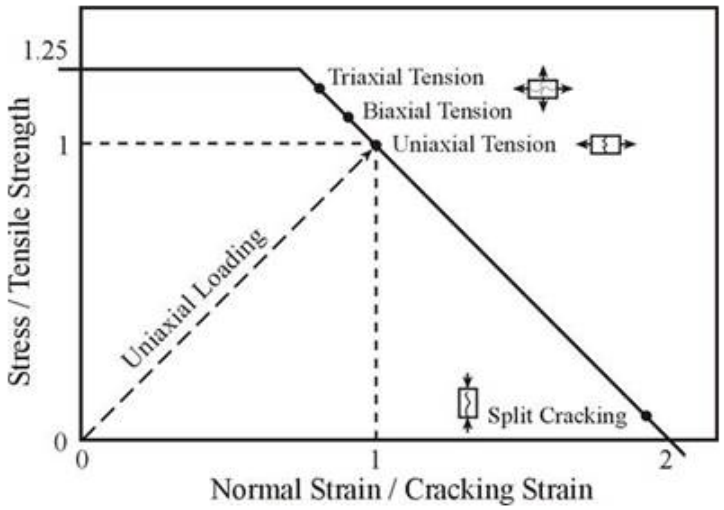

Figure 2 Crack Initiation Criteria Curve

SINGLE ELEMENT TEST CASES

Single element test case analyses were performed to validate the capability of the ANACAP concrete model. A one-inch cube element was used with using realistic, but arbitrary, material properties. Both static and time-dependent mechanical properties were utilized during this series of analyses. The ANACAP concrete material model was utilized with no time dependent properties. Various boundary conditions are imposed:

1. ***Unconfined***: Zero displacement on -X, -Z, and -Y faces. Pressure (2ksi compression) imposed on +Y face.
2. ***Partially Confined***: Zero displacement on -X, +X, -Z, and -Y faces. Pressure (2ksi compression) imposed on +Y face.
3. ***Confined***: Zero displacement on -X, +X, -Z, +Z, and -Y faces. Pressure (2ksi compression) imposed on +Y face.
4. ***Unconfined with Imposed Displacement***: Zero displacement on -X, -Z, and -Y faces. Impose 5e-4in displacement (equivalent to 2ksi compression) on +Y face.

Initially these four test cases were analyzed with static mechanical properties for elastic modulus and creep compliance. In each of the three pressure tests (1-3) the pressure is applied, the analysis steps through time for a simulated 30 years (creep), the pressure is removed, and the element strains are allowed to recover (creep recovery). In the imposed displacement test (4) the imposed displacement is applied, the analysis steps through time (creep), the imposed displacement is removed (i.e., an imposed displacement of 0 in is applied), and the element strains are allowed to recover (creep recovery).

The three pressure tests show no element cracking and strains (both axial and transverse) that align with theoretical estimates. This illustrates and confirms that “unrestrained” creep and creep recovery as a visco-elastic process, do not generate mechanical or cracking strains, that is, if the imposed mechanical stress/strain do not induce cracking, then visco-elastic formulated creep affects the total strain but not the mechanical strain. When the material is allowed to unload back along the same path or same conditions as when loaded, then no cracking develops due purely to creep strain. Creep strain can affect the mechanical strain when this unloading path or stress conditions have changed during the creep accumulation. The imposed displacement test illustrates this point. Here, the results also align with theory but show cracking

when the imposed displacement is removed. This result is expected; imposing zero total strain requires a tensile mechanical strain to develop to balance the compressive creep strain.

The unconfined pressure test, case 1, was repeated with time dependent elastic modulus and creep compliance activated in the constitutive model using three variations. The first case only included the time dependence for the modulus of elasticity. Figure 3 shows the axial strain (negative = compression) when a pressure is applied at time zero and then removed after 30 years. Because the modulus has increased over time the element does not return to a zero-strain state upon unloading. For the second variation, both time dependent modulus and creep are included in the sample problem. The results are presented in Figure 4. Note that when a time dependent modulus is included in the assessment there is less strain recovered during the creep recovery phase. This result is in-line with that shown in Figure 3. The third variation applied the pressure load periodically in time (i.e., the load is applied instantaneously then removed). The resulting axial strain is shown in Figure 5 and decreases in time (as the modulus increases with time); the results match those calculated from theory.

In summary, these test cases subject the element to an arbitrary compressive load, holds the load constant for 30 years, and then releases the load. The load initially displaces the element by an axial strain of 500 με. Unloading the element after 30 years, including an aging elastic modulus, returns the element to an axial strain of 95 με. Because the elastic modulus has increased with age, the concrete element does not return to zero strain upon unloading. Similarly, the creep modulus of concrete decreases as concrete ages; young concrete subjected to a given load will creep more over time than old concrete subjected to the same given load. The single-element simulations also exemplify the effect of a time-dependent modulus, indicating that aging concrete will creep less than young concrete.

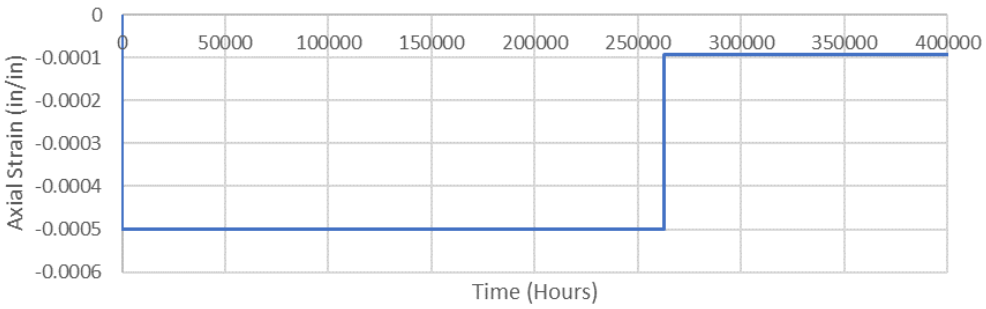

Figure 3 Non-Recoverable Displacement, Time Dependent Modulus Only

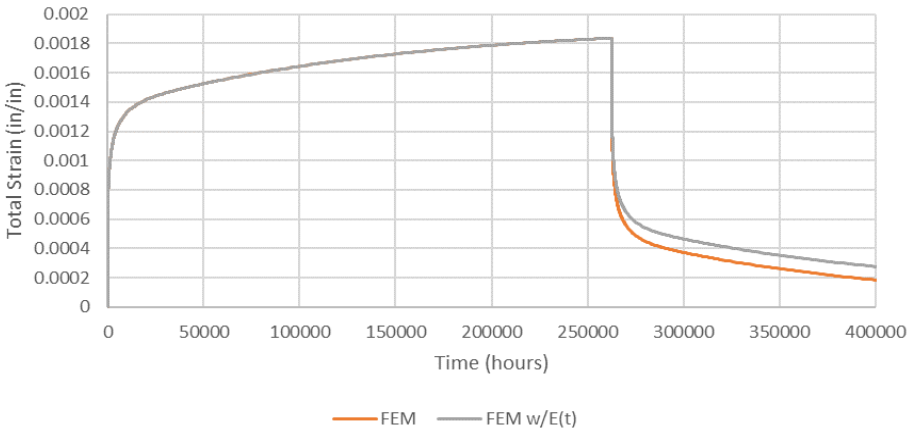

Figure 4 Creep with Time Dependent Modulus

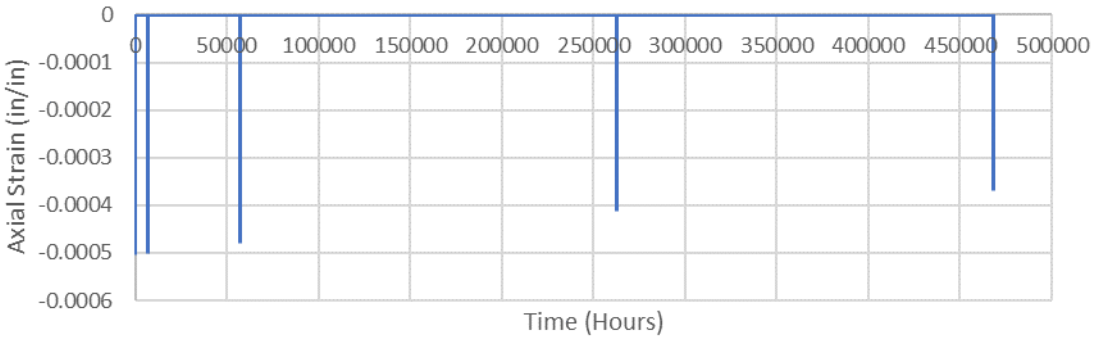

Figure 5 Periodic Loading with Time Dependent Modulus

MODEL OF CONTAINMENT STRUCTURE

A representative containment structure was used in this part of the study. A general schematic showing the region of interest and the corresponding FEA mesh is shown in Figure 6.The structure is modeled with quarter symmetry. A vertical boundary (D_y=0) is included at the base of the model while a circumferential boundary (q=0in) is included at the buttress and containment wall. The explicitly modeled rebar, tendons and boundary surfaces are illustrated in Figure 7. Key components of the model are summarized below.

- **Buttresses:** The model assumes six vertical buttresses equally spaced along the circumference. The buttresses are 6ft ft wide and 5ft-10in thick. The buttresses are modeled as elastic with a Young's Modulus of 4e6psi (the ANACAP material model is not applied to the buttress).
- **Ring Girder**: The model includes a 6ft tall, 5ft-10in thick girder at the top of the panel to represent the ring girder (or the stiffened equipment hatch in the quarter-symmetric model). The girder is modeled as elastic with a Young's Modulus of 8e6psi (the ANACAP material model is not applied to the ring girder). Note that this Modulus is a factor of 2 greater than the other concrete components to account for additional stiffness provided by the adjacent concrete elements not explicitly modeled.
- **Steel Liner:** A 3/8in steel liner (modeled as a membrane) is bonded to the inner diameter of the structure. The liner is modeled as elastic plastic (fy=50ksi, fu=75ksi at 20% strain) with a Young's Modulus of 30e6psi.
- **Containment Wall:** The containment wall is modeled as 3.5ft thick and is modeled with the ANACAP concrete constitutive model. Unless otherwise stated, the concrete is assumed to have a 5ksi strength, 4e6psi Youngs Modulus, and 0.2 Poisson's ratio. The containment wall is modeled with quadratic solid elements (C3D20R).
- **Containment Wall Reinforcement:** The containment wall includes vertical and horizontal reinforcement. The reinforcement is modeled as elastic plastic (fy=60ksi, fu=70ksi at 10% strain) with a Young's Modulus of 29e6psi. The horizontal rebar is modeled as #9@12in each face. The vertical rebar is modeled as #9@10in each face. Rebar is modeled as linear truss elements (T3D2). Tie bars (stirrups) are not included in the model. The reinforcement is embedded in the concrete through an embedment constraint providing strain compatibility between the concrete and rebar.
- **Containment Wall Tendons:** The containment wall includes vertical and horizontal tendons. The tendons are modeled as elastic plastic (fy=200ksi, fu=235ksi at 10% strain) with a Young's Modulus of 28e6psi. Both horizontal and vertical tendons have a cross sectional area of 10.9in^2. Vertical tendons are spaced radially every 2.5degrees, which roughly equates to a 35.2in circumferential spacing. Horizontal tendons are located in alternating layers spaced at 12.75in and

25.5in respectively. The vertical and horizontal tendons are located 15.2in and 10in from the containment wall outer radius, respectively. The tendon prestress is applied through an imposed temperature change of 810°F, which for a 6.5e-6 in/in/deg F expansion coefficient, equates to 5.27e-3 in/in or 147ksi or 1600 kip per tendon. This roughly equates to 1ksi and 2ksi compression in the vertical and horizontal directions, respectively. The tendon force is not altered to account for friction, wobble, steel relaxation, etc. The tendons are embedded in the concrete through an embedment constraint and are modeled as linear truss elements (T3D2). No reduction in concrete area (accounting for tendon ducts) is included.

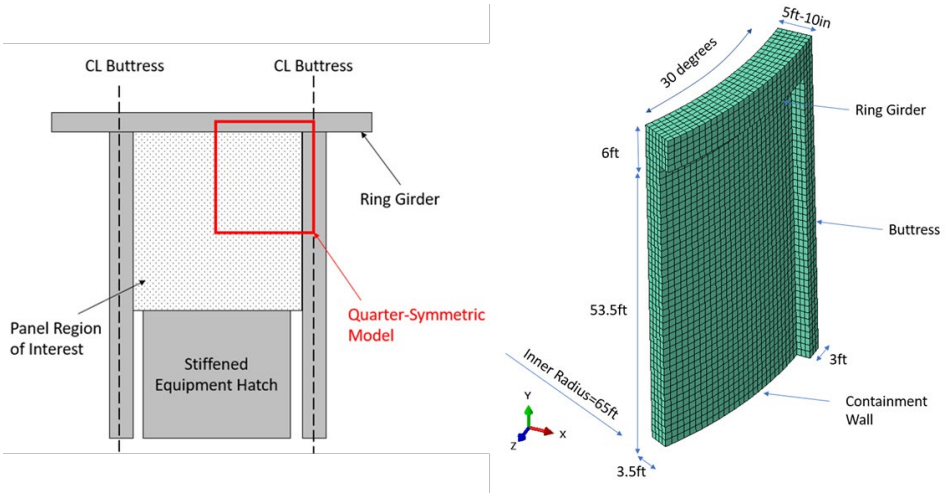

Figure 6 Schematic of Region of Interest (left), Representative FEM Mesh

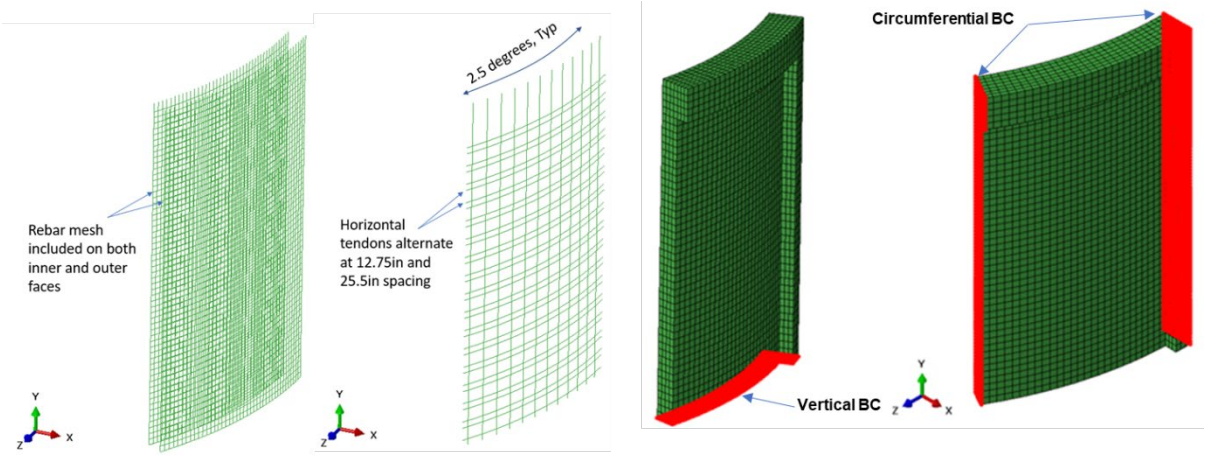

Figure 7 Explicit Layout of Reinforcement Steel, Tendons, and Boundary Conditions

Each analysis is segregated into multiple analysis steps. The first steps apply gravity and the tendon tensioning force. The analyses are then permitted to run through the creep steps that span ~30 years. At the end of ~30 years several tendons (both horizontal and vertical) are removed to represent the de-tensioning that would occur before an equipment opening would be cut into the containment wall. The tendons that are de-tensioned are shown in Figure 8 with the approximate location of the proposed equipment opening also highlighted. These analyses do not include effects of cutting the opening. The tendons are both tensioned and de-tensioned by applying a temperature load to the tendon elements.

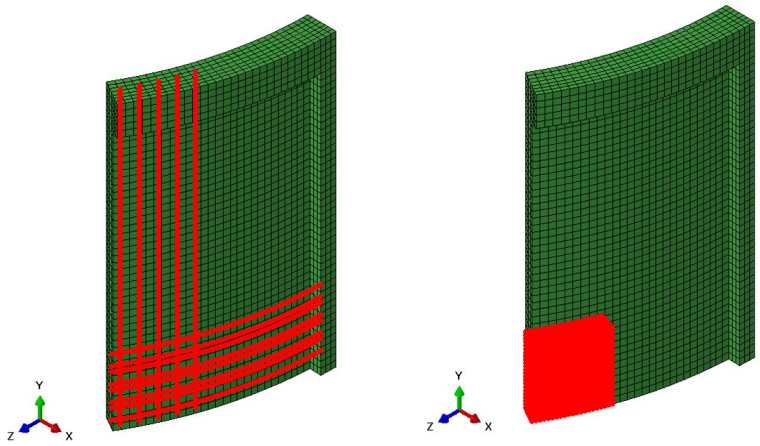

Figure 8 FEM – De-tensioned Tendons (Left) and Future Concrete Opening (Right)

SUMMARY OF SELECTED ASSESSMENTS AND FINDINGS

Twenty-one analysis variations were considered in this study. Variables considered included concrete fracture strain, creep compliance factors, differential creep, time dependent concrete material properties, and tendon removal sequence. Due to the space limitations only select key results are presented as summarized in Table 1.

Table 1 Summary of Analyses

Case
Case A1 – Baseline, No Creep
Case A2 – Baseline, With Creep
Case B1 – Delamination During Initial Tensioning, With Creep
Case B2 – Investigating Potential Delamination After Initial Tensioning

Comparison Baseline With and Without Creep (Cases A1 and A2)

Without creep active (Case A1) the detensioning has resulted in a radial outward displacement near the region of the future concrete opening, as can be seen in Figure 9. The maximum radial strain at the end of the detensioning step is 161.1e-6 in/in but with a significant change in strain contour shown in Figure 10. The analysis indicates cracking of the concrete has occurred at the end of the detensioning step. Since the radial strain is less than twice the fracture strain, cracking is believed to be occurring due to flexural stress (stemming from the effects of the de-tensioned tendons), concentrated near the future opening and the inner diameter (near the ring girder). With creep active (Case A2) no cracking is observed after 30 years of creep (prior to de-tensioning). Since cracking is not evident prior to de-tensioning, the increase in radial strain prior to de-tensioning is attributed to the development of creep strain (as opposed to increased mechanical strain). Note that the radial strain profile after de-tensioning when creep is included now resembles the hourglass shape seen in the delamination cracking in the Crystal River containment. Figure 11 shows the radial strain just before and after de-tensioning for the two cases, and after 5250 hours of creep recovery.

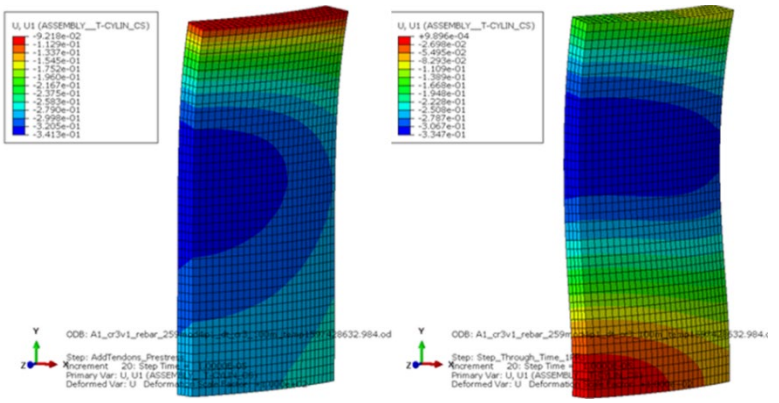

Figure 9 Radial Displacement, Case A1, After Initial Stressing (Left) and After Detensioning (Right)

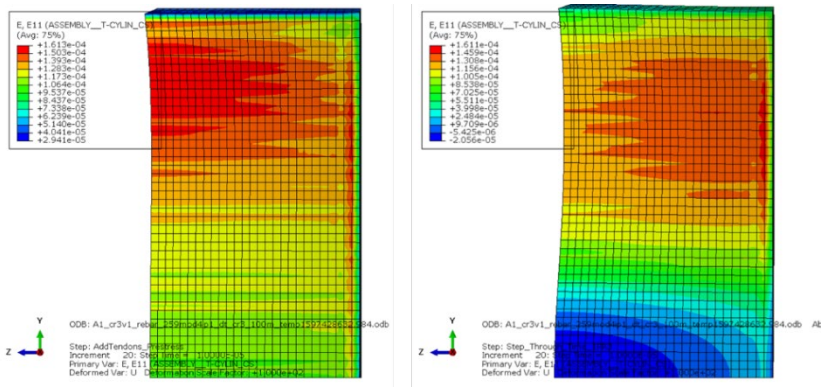

Figure 10 Radial Strain, Case A1, After Initial Stressing (Left) and after Detensioning (Right)

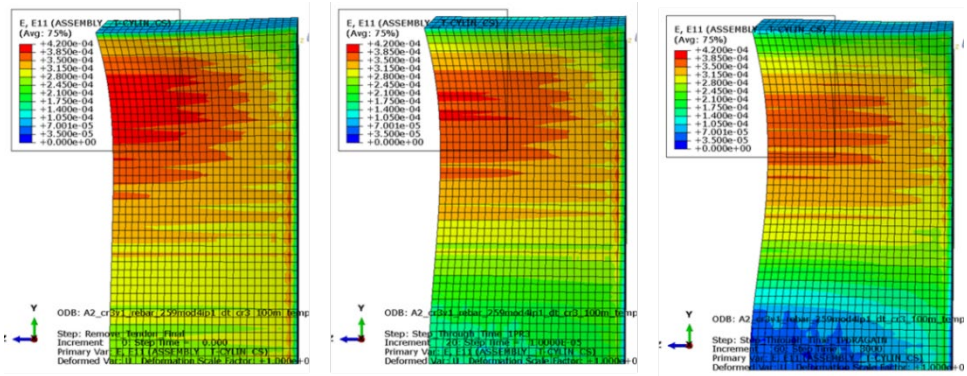

Figure 11 Radial Strain Case A2, Before Detensioning (Left), After Detensioing (Center), 5250 Hours Creep Recovery (Right)

Delamination at end of Initial Tensioning (Case B1)

In this analysis the concrete tensile strain limit is adjusted such that cracking of the containment wall occurs at the end of the initial tensioning phase (i.e., at 0 years). This assessment is performed to observe how the inclusion of a crack in the containment wall might propagate because of creep. Cracking occurs during the last increment of tendon stressing and quickly propagates at the outer diameter. The cracking

starts near the highest radial strain and propagates from this location following the radial strain pattern seen in Figure 10. The radial strain shown in Figure 12 shows the propagation of cracking within the PCCV panel. Note that the delaminated nodes appear concentrated at the outer diameter of the structure. The analysis was discontinued prior to the creep steps as the structure has obviously failed due to tensioning. The simplified modelling used in this case has an inherent brittle failure mode since there is no alternative load path when mechanical loading causes delamination due to radial strains. This result also provides confidence that the modelling used is fully capable of capturing the delamination cracking if conditions warrant.

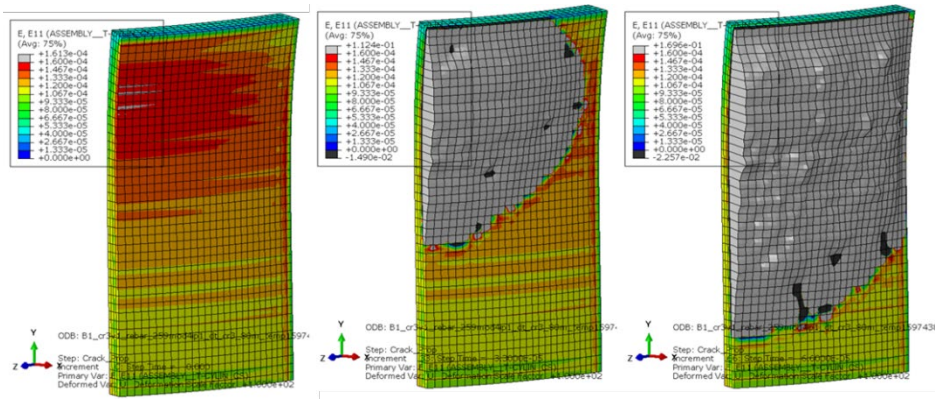

Figure 12 Crack Propagation After Initial Stressing

Investigating Potential Delamination After Initial Tensioning

In this analysis the concrete tensile strain limit is set slightly higher than that in Case B1 to prevent delamination during initial tensioning. This assessment is performed to observe if a delamination crack will form due to creep or creep recovery when a low tensile strength concrete is assumed. Associated radial strain contours are shown in Figure 13. At the end of the initial stressing step 929 integration points are near cracking (>90% likelihood), although no cracking has occurred. After 250 hours of creep, only 41 integration points are near cracking, indicating that creep is reducing the likelihood of cracking. No cracking is observed prior to de-tensioning. De-tensioning appears to cause the formation of flexural cracks near the future opening and inner diameter (near the ring girder). Approximately twice as many cracks form in Case B2 when compared to Case A2. This is attributed to the lower concrete fracture strain used in Case B2. It is not apparent that radial delamination has occurred. The total number of cracks observed during the creep recovery steps is not seen to change significantly, indicating crack propagation is not occurring.

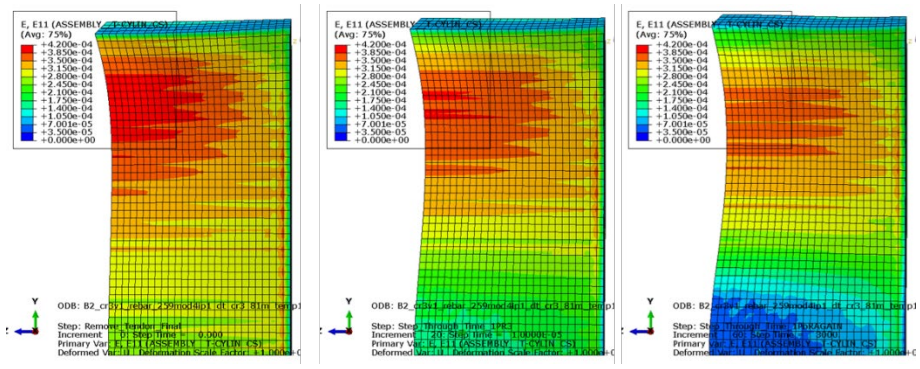

Figure 13 Radial Strain Case B2, Before Detensioing (Left), After Detensioing (Center), 5250Hr Creep Recovery (Right)

CONCLUSIONS

This study was performed as a proof of concept to show the analytic viability to model the long-term creep response in concrete and its effects in PCCV's. In summary, the radial strain profile after detensioning is significantly different if creep is included in the analysis (Case A1 vs A2) and the profile with creep better resembles the hourglass shape found in the delamination cracking pattern at Crystal River. A sufficiently large concrete fracture strain capacity is required during initial tendon stressing or delamination may occur (Case B1) due to radial tensile strains that develop on the outer side of hoop tendons. Delamination, when it occurs, appears to follow the radial strain contour which is observed in actual delamination failures. After initial stressing, creep appears to reduce the radial mechanical strain, resulting in a lower likelihood of delamination (Case B2). While not included herein due to space limitations additional findings from this study Identified the following.

If a local defect is introduced just after initial tensioning (i.e., early in the creep analysis), there may still be sufficient mechanical strain demand to cause widespread delamination. If a local defect is introduced significantly after initial tensioning (6.5 years after initial tensioning, just prior to detensioning, or immediately after detensioning, a cascading delamination event was not observed.

Removing the horizontal tendons while leaving the vertical tendons in place shows an increase in mechanical radial strain after detensioning and an increase in total radial strain during the creep recovery steps. The effects of creep coupled with the sequence and timing of tendon detensioning may play a role in exacerbating delamination cracking.

Differential creep analyses, wherein a lower creep factor was assigned to the outer concrete elements, caused a delamination failure to occur during the creep steps. The outer diameter concrete elements appear to act as a displacement restraint, leading to the development of mechanical strain as the interior concrete elements creep inwards.

At this time additional research and analytic tool development, sponsored by the United States Nuclear Regulatory Committee, is going on in a collaborative effort between Sandia National Lab, Structural Integrity Associates, Structural Solutions Consulting and the NRC to further the understanding of long-term creep effects in PCCV's.

REFERENCES

Dassault Systemes. (2018). ABAQUS Analysis User's Guide 6.18. *DS Simulia.*

Rashid Y.R., Dunham R.S., James R.J. (1998) *ANACAP Concrete and Steel Constitutive User Routine 2.59 User and Theory Manuals*. Anatech Corporation

Rashid Y.R., Dunham R.S., James R.J. (2010) *Modeling and Analysis of Aging Behavior of Concrete Structures in Nuclear Power Plants*. Fontevraud 7 International Symposium, Avignon, France, September, A088 T10.

Kjolsing E., James R.J. (2020) *Creep Effects in PCCVs*. Structural Integrity Associates Inc. Report No. 1901160.401.R0 for Sandia National Laboratory.